Thermal Science and Engineering Progress 42 (2023) 101934

Contents lists available at ScienceDirect

Thermal Science and Engineering Progress

journal homepage: www.sciencedirect.com/journal/thermal-science-and-engineering-progress

Use of Nano-Encapsulated phase change material mixed with water for natural convection cooling in combination with nickel foam

Kamel Guedri [a,1], Fahid Riaz [b], Bandar M. Fadhl [a], Manoj Kumar Agrawal [c], Nehad Ali Shah [d,1], Basim M. Makhdoum [a], Hossein Mehdizadeh Youshanlouei [e,*]

[a] *Mechanical Engineering Department, College of Engineering and Islamic Architecture, Umm Al-Qura University, P. O. Box 5555, Makkah 21955, Saudi Arabia*
[b] *College of Engineering, Abu Dhabi University, Abu Dhabi, United Arab Emirates*
[c] *GLA University, Mathura (UP) 281406, India*
[d] *Department of Mechanical Engineering, Sejong University, Seoul 05006, South Korea*
[e] *Sustainable Management of Natural Resources and Environment Research Group, Faculty of Environment and Labour Safety, Ton Duc Thang University, Ho Chi Minh City, Viet Nam*

A R T I C L E I N F O

Keywords:
CFD
Free convection
Nickel foam
NEPCM
n-Docosane

A B S T R A C T

This study investigated the potential benefits of using free convection mechanisms to cool parts, as opposed to forced convection mechanisms that require energy to transfer heat and mass. The research team cooled a hot plate, which had a uniform heat flux, by utilizing the free convection flow inside a square cavity. They also installed a partial nickel porous media with different porosities on the hot plate and injected nano-encapsulated phase change material (NEPCM) particles into water to form a cooling fluid mixture. For the NEPCM particles, the researchers selected n-docosane with a melting temperature of 317.65 K for the core and polyurethane for the shell. The researchers used computational fluid dynamics (CFD) to simulate the cooling process with varying parameters, including porosity, deflection angles, and NEPCM volume fraction. The results showed that the cooling performance of nickel foam was significantly better than that of NEPCM. For example, when the porosity of the nickel foam decreased from 0.98 to 0.93, the average Nusselt number increased by 142 %, indicating a considerable improvement in cooling efficiency. In comparison, increasing the NEPCM volume fraction from 0 to 6 % only resulted in a modest 5.6 % increase in the average Nusselt number.

Introduction

One of the major challenges faced by industries such as foundry, steel, forging, sheet metal, and electronics is the cooling of hot parts and devices [1-3]. In these industries, mechanical or electronic components may be in operation that come in contact with heating processes, or they may generate heat due to mechanical friction or electric dissipation. If the temperature of these components is not kept within a safe range, they can be damaged or destroyed. As a result, thermal engineers must design appropriate cooling systems to maintain safe operating temperatures [4-6]. In recent years, researchers across various fields have been seeking systems that minimize air and noise pollution, environmental impact, and cost. As a result, thermal engineers have turned their attention to natural convection as a heat transfer mechanism, as it does not require any pump or piping systems unlike forced convection [7-9]. In most cooling systems, a fluid is necessary to receive heat from a part and release it outside, requiring a driving force to move it. Forced convection uses a pump to generate this driving force, but free convection does not require such a device [10-12]. The Buoyant force, one of the oldest forces in fluid science, is observed due to differences in density of a solid or fluid within another fluid. This force also occurs within a fluid due to differences in density resulting from concentration or temperature gradients, provided that the solute density differs from the solvent density and the fluid has a suitable thermal expansion coefficient that changes in temperature lead to changes in fluid density [13-15]. Free convection relies on Buoyant force generated by density changes due to temperature differences, which move the heated fluid away from the part to cool it down. The driving force must be sufficient to overcome viscous forces and accelerate the fluid [16]. Thermal engineers have been exploring innovative methods to improve cooling

* Corresponding author.
E-mail address: hossein.mehdizadeh.y@gmail.com (H. Mehdizadeh Youshanlouei).
[1] These authors contributed equally to this work and are co-first authors.

https://doi.org/10.1016/j.tsep.2023.101934
Received 11 April 2023; Received in revised form 8 May 2023; Accepted 26 May 2023
Available online 27 May 2023

efficiency beyond the use of a single cooling fluid. These methods include embedding a porous medium and adding nanoparticles to the cooling system [17-19]. Metal porous media with pores can increase the contact surface area of heat exchange with the fluid and have high thermal conductivity, making them a popular choice for installation on hot parts. Mesgarpour et al. [20] used porous media with 0 to 0.7 porosity to cool a photovoltaic panel, demonstrating a 15 % increase in heat transfer rate. However, another study [21] that used porous media for cooling a concentrator photovoltaic system found destructive effects on system performance. Additionally, studies [22-24] have employed porous media for cooling a CPU by heat pipe, in a solar thermoelectric energy harvesting system, and inside a vehicle radiator. Phase change material (PCM) is a substance that can absorb and release thermal energy during the process of changing its physical state, such as from solid to liquid or liquid to gas. This property makes PCMs useful in thermal energy storage applications, where they can store thermal energy during periods of excess heat or cold and release it when needed. PCMs are often used in building and construction materials, such as insulation and concrete, as well as in thermal management systems for electronic devices and vehicles. The use of PCMs can help reduce energy consumption and costs, and contribute to more sustainable and efficient energy practices [25-27].

The use of micro- and nano-sized capsules containing phase change materials (PCMs) in solid–liquid phase transition is a popular method in recent thermal engineering studies, referred to as micro- and nano-encapsulated PCMs (NEPCMs) [28]. According to a study [29], encapsulating PCMs enables the utilization of their latent heat capacity during melting. Because the phase change process inside capsules occurs at a constant temperature, the mixture of host fluid and NEPCMs can receive heat as both sensible and latent heat from the hot source simultaneously, at a lower temperature than pure fluid. This results in increased temperature gradient between the hot part and the fluid, which is a crucial parameter in studying heat transfer rate in thermal engineering [30]. Saleh et al. [31] demonstrated that adding 1 % volume fraction of NEPCM into a base fluid can enhance heat transfer rate by 9 % in natural convection mechanisms inside an asymmetrical U-shaped enclosure. Raizah et al. [32] used NEPCM inside a porous enclosure to study free convection, while Lan et al. [33] prepared NEPCM with n-Octadecane as the core and SiO2/BN as the shell, leading to a 5-fold increase in thermal conductivity and a 12.1 °C reduction in hot source temperature with 20 % weight. Additionally, many recent studies [34-36] have employed NEPCM to improve the performance of various systems.

This study aims to investigate the use of free convection mechanisms to cool a hot part by reviewing past research in thermal engineering. The hot part was modeled as a flat plate with a constant heat flux, installed at the bottom of a square cavity capable of inclination. A porous metal block made of nickel was embedded on the hot plate. In contrast to previous studies, this study adds NEPCM with n-Docosane core and a melting temperature of 317.65 K to water. The problem was simulated using computational fluid dynamics (CFD) based on the finite volume method (FVM) to examine the effects of porosity, deflection angle, and volume fraction of NEPCM on temperature, velocity, melting contours, and Nusselt number at a Rayleigh number of 10^5.

Illuminating the problem

To better understand the following descriptions, Fig. 1 depicts the present problem, which involves a square cavity with dimensions of $L \times L$ placed on a flat plate with a length of $0.5L$. A uniform heat flux of q'' is emitted to the plate, while the other three cavity walls, including the left, right, and top walls, were maintained at temperature T_C. A nickel foam with dimensions of $0.25L \times 0.5L$ was placed on the flat plate to increase the heat transfer exchange area. The chamber was filled with water as the base fluid and NEPCM as the suspension, which the core and shell of the NEPCM made of n-Docosane with a melting temperature of 317.65 K and polyurethane, respectively. As explained in the

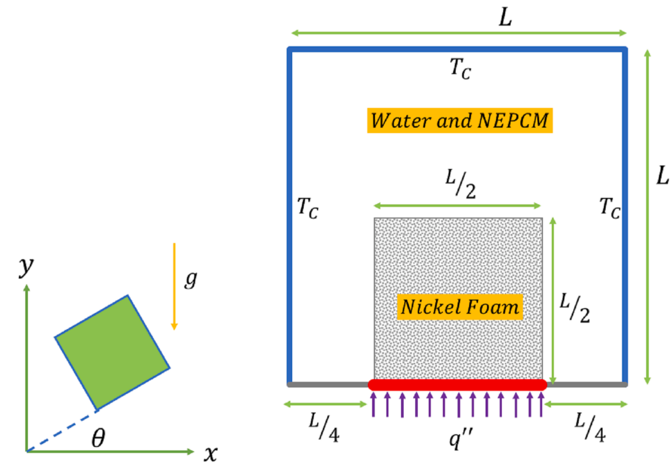

Fig. 1. The schematic of a cavity, including partial porous media with details.

introduction, the hot flat plate was cooled using a free convection mechanism, with the hot and cold sources being the flat plate and the cavity walls, respectively. The cavity had the ability to rotate counter-clockwise by an angle of θ, and in all cases, the gravitational acceleration (g) was in the negative y-direction.

Hypothesis and conservation equations

To solve any CFD problem, it is first necessary to present the governing equations in accordance with the hypotheses. In this study, the considered hypotheses include steady, laminar, incompressible, 2-dimensional, thermal equilibrium water with NEPCM particles and porous medium, regardless of shape change of NEPCM, and constant properties. In this problem of free convection, equations of mass, momentum and energy conversation are coupled and also the effects of Darcy force are taken into account in the equation of momentum. Hence, the governing equations in the x-y coordinates are as follows [37]:

Mass conservation:

$$\frac{\partial u}{\partial x}+\frac{\partial v}{\partial y}=0. \tag{1}$$

Momentum conservation:

$$\frac{\rho_m}{\varepsilon^2}\left(u\frac{\partial u}{\partial x}+v\frac{\partial u}{\partial y}\right) = -\frac{\partial p}{\partial x}+\frac{\mu_m}{\varepsilon}\left(\frac{\partial^2 u}{\partial x^2}+\frac{\partial^2 u}{\partial y^2}\right)-\frac{\mu_m}{K}u+(\rho\beta)_m(T-T_C)g sin\theta \tag{2}$$

$$\frac{\rho_m}{\varepsilon^2}\left(u\frac{\partial v}{\partial x}+v\frac{\partial v}{\partial y}\right) = -\frac{\partial p}{\partial y}+\frac{\mu_m}{\varepsilon}\left(\frac{\partial^2 v}{\partial x^2}+\frac{\partial^2 v}{\partial y^2}\right)-\frac{\mu_m}{K}v+(\rho\beta)_m(T-T_C)g cos\theta \tag{3}$$

Energy conservation:

$$u\frac{\partial}{\partial x}\left(\rho_m C_{P,m}T\right)+v\frac{\partial}{\partial y}\left(\rho_m C_{P,m}T\right)=k_{eff}\left(\frac{\partial^2 T}{\partial x^2}+\frac{\partial^2 T}{\partial y^2}\right). \tag{4}$$

Which $uandv$ are the velocity in $xandy$ directions, respectively. Also, $p, K, T, andg$ denote pressure, permeability, temperature, and gravitational acceleration, respectively. Moreover, $\rho, \mu, \varepsilon, \beta, C_p, andk$ describe density, dynamic viscosity, porosity, thermal expansion coefficient, specific heat capacity, and thermal conductivity, respectively. First of all, the NEPCM's core was n-Docosane (C_{22}) with fusion temperature (T_f) of $317.65K$, melting temperature range (T_{mr}) of $0.4K$, and latent heat (h_f) of $249\frac{kJ}{kg}$. Hence, the thermophysical properties of NEPCM such as density, thermal conductivity, specific heat capacity, and thermal expansion by regarding the both thermophysical properties of core and shell can be computed according to Table 1.

Table 1
The thermophysical properties of NEPCM [37].

Properties name	Formula
ρ_{np}	$\frac{(1+\omega)\rho_c\rho_s}{\rho_s+\omega\rho_c}$
k_{np}	$\frac{d_s}{\frac{d_c}{k_c}+\frac{d_s-d_c}{k_s}}$
d_c	$d_s\left(\frac{\rho_s}{\rho_s+\omega\rho_c}\right)^{1/3}$
$C_{p,np}$	$\frac{(C_{p,c}+\omega C_s)\rho_c\rho_s}{(\rho_s+\omega\rho_c)\rho_{np}}$
$C_{p,c}$	$C_{p,l}+\left\{\frac{\pi}{2}\left(\frac{h_f}{T_{mr}}-C_{p,l}\right)\left(\sin\pi\frac{T-(T_f-T_{mr}/2)}{T_{mr}}\right)\right\}\times \begin{cases} 0 if T < T_f-\frac{T_{mr}}{2} \\ 1 if T_f-\frac{T_{mr}}{2} < T < T_f+\frac{T_{mr}}{2} \\ 0 if T < T_f+\frac{T_{mr}}{2} \end{cases}$
β_{np}	$\beta_c+\left(\frac{\beta_s-\beta_c}{2}\right)\left(1-\frac{\omega\rho_s}{\rho_c}\right)$

Which ω is mass ratio of shell to core, which equals 0.7 in this study. Moreover, the used material for shell was polyurethane with diameter (d_s) of $100nm$. Moreover, the thermophysical properties of mixture by considering water and NEPCM including density, thermal conductivity, dynamic viscosity, specific heat capacity, and thermal expansion can be calculated according to Table 2.

To compute the thermophysical properties of NEPCM and mixture need the thermophysical properties of n-Docosane, polyurethane, and water, which are arranged in Table 3. Moreover, the permeability of nickel foam was $8.7\times10^{-4} and 10.1\times10^{-4}$ for $\varepsilon = 0.93 and 0.98$, respectively. Also, the effective thermal conductivity of mixture and porous media, where the nickel foam was presence, was set $4.11 and 1.68$ for $\varepsilon = 0.93 and 0.98$, respectively. These value of permeability effective thermal conductivity was computed based on study [38]. Eventually, in all formulas, the subscripts of $m, c, s, f and np$ show the mixture, core, shell, water, and NEPCM, respectively.

The boundary conditions on walls for momentum equations was set no slip. Moreover, the boundary conditions on hot plat and cavity walls were set uniform heat flux of $q'' = 300\frac{W}{m^2}$ and uniform temperature of T_c, respectively. In this study, the Rayleigh number of base fluid for calculating g by considering $L = 1m$ and Nusselt number are computed as following:

$$Ra = \frac{g\beta_f q'' L^4}{k_f\alpha_f v_f} \tag{5}$$

$$Nu_{avg} = \frac{2}{k_m}\int_{0.25L}^{0.75L}\frac{q''}{(T_p-T_c)}dx \tag{6}$$

Table 2
The thermophysical properties of mixture of water and NEPCM [37].

Properties name	Formula
ρ_m	$(1-\varphi)\rho_f+\varphi\rho_{np}$
k_m	$\frac{k_{np}+2k_f+2\varphi(k_{np}-k_f)}{k_{np}+2k_f-\varphi(k_{np}-k_f)}k_f$
$C_{P,m}$	$\frac{(1-\varphi)\rho_f C_{Pf}+\varphi\rho_{np}C_{P,np}}{\rho_m}$
β_m	$\frac{(1-\varphi)\rho_f\beta_f+\varphi\rho_{np}\beta_{np}}{\rho_m}$
μ_m	$\frac{\mu_f}{(1-\varphi)^{2.5}}$

Table 3
The thermophysical properties of n-Docosane, polyurethane, and water.

Properties	Water	n-Docosane	Polyurethane
$\rho\left(\frac{kg}{m^3}\right)$	996	880	786
$k\left(\frac{W}{mK}\right)$	0.62	0.205	0.025
$C_P\left(\frac{J}{kgK}\right)$	4180	2000	1317
$\beta\left(\frac{1}{K}\right)\times10^{-5}$	21	50	17.3
$\mu\left(\frac{kg}{ms}\right)\times10^{-6}$	795	–	–

Which T_p is the local temperature of hot plat.

CFD method and verification

Computational fluid dynamics (CFD) contributes to simulate the variety phenomena that deals with flow. Finite volume method is more practical among other methods in CFD such as finite difference method (FDM), finite element method (FEM), Lattice Boltzmann method (LBM), smoothed particle hydrodynamics (SPH), and spectral method (SM). Hence, this study was simulated by means of FVM based on SIMPLE algorithm. The pressure and velocity need to be coupled with each other in FVM method to correct fields. In addition, the upwind and central schemes were implemented to discretize divergence and Laplacian terms in momentum and energy equations, which these schemes have second-order accuracy [12,39-46]. Besides, the structured mesh-square cells-was used to mesh the cavity in order to be simple the geometry. Finally, many mesh numbers must be investigated to be independent of the results from mesh numbers. So, Fig. 2(a) represents the value of average Nusselt number versus mesh number at conditions 0.93 porosity, 0 deflection angle, and 0.06 vol fraction of NEPCM to study the independent of the results from mesh numbers. The results of Fig. 2(a) shows that the variation of average Nusselt number from 140*140 to 200*200 is less than 1.2 % compared with from 100*100 to 140*140 and from 200*200 to 240*240. As result, the mesh 80*80 could be good selection in this study.

Study of Golab et al. [37] have been used to verify the implemented code. They encapsulated the n-nonadecane within polyurethane shell and injected into water for enhancing the performance of natural convection inside a square cavity. So, their results for average Nusselt number at conditions of $\chi = 100, \delta = 0.3, and \theta_f = 0.5$ was used to compare results of present study, which are illustrated in Fig. 2(b). According to Fig. 2(b), the maximum error between result is 2.1 %, which occurs in 3 % volume fraction of NEPCM.

Results and discussion

The different important parameters including porosity, deflection angle, and volume fraction of NEPCM at 10^5 Rayleigh number was simulated to study the magnitude velocity, temperature, and molten NEPCM contours, distribution of temperature on hot plat, and average Nusselt number that are deeply analyzed in this section. Fig. 3 shows the magnitude velocity and temperature contours at conditions of the 0.93 porosity and the 6 % volume fraction of NEPCM for different deflection angles. According to the deflection angle of 0 and the magnitude velocity contour, it can be said that the two stretched vortices of clockwise and counterclockwise in vertical direction can be seen in the right and left halves of the cavity, respectively. In addition, the magnitude velocity near the vertical walls is higher than other points because the sides of the vertical walls do not have a porous medium to reduce the magnitude velocity due to Darcy force. On the other hand, the lowest velocity is seen inside the porous medium because the porous medium is the cause of a pressure force against the motion of the flow. Increasing

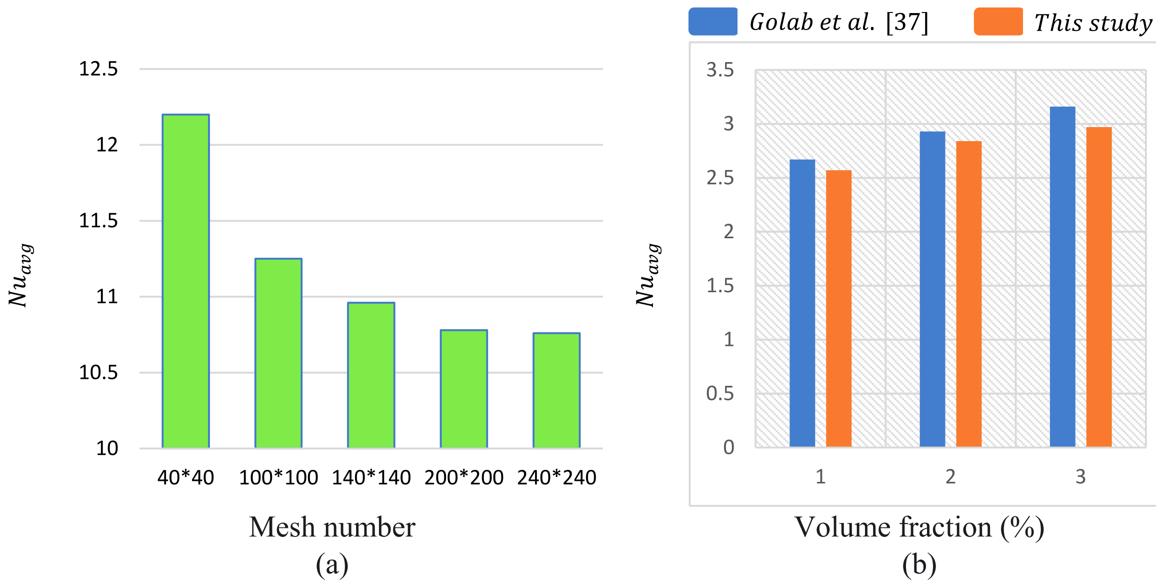

Fig. 2. Two Bar plots for a) mesh independency for average Nusselt number and b) verification the used code with results of Golab et al. [37].

the deflection angle from 0 to 30 causes the maximum flow velocity to be observed on the left wall and it escalates the maximum flow velocity by 56 %. Furthermore, increase of the deflection angle to 60, the highest flow velocity occurs in the left and upper walls and the maximum velocity has been increased by 91 % compared to the deflection angle of 0. Finally, increasing the deflection angle to 90, the highest flow velocity is appeared in the 4 sides of cavity walls, and the maximum velocity has been increased by 98 % relative to the deflection angle of 0. A noteworthy point is observed in increasing the deflection angle is that increasing the flow velocity inside the porous medium near the hot plate is directly related to increasing the deflection angle from 0 to 90. According to the temperature contour at the deflection angle of 0, the isotherms near the hot plate are in the form of a half-elliptic with the larger diameter that tend to be a half-elliptic with small diameter by moving away from the hot plate. This ellipticity of isotherms is due to two reasons: firstly, the three cavity walls act as cold sources that satisfy the essence of the PDE energy equation (Eq. (2). Secondly, the nickel porous medium penetrates the heat very quickly into the flow, which does not allow the heat to penetrate farther away from the hot plate for increasing temperature. Also, increasing the deflection angle has no effect on the isotherms and the maximum temperature because the increment of effective thermal conductivity due to the nickel foam prevails to the effects of changing the flow pattern with the deflection angle.

Fig. 4 illustrates the magnitude velocity and temperature contours at conditions of the 0.93 porosity and the 6 % volume fraction of NEPCM for different deflection angles. It can be implied that the arguments in Fig. 3 are true for Fig. 4 except for the effects of the deflection angle on the temperature contours. By comparing Figs. 3 and 4, increasing the porosity from 0.93 to 0.98 increases the maximum flow velocity by 167 %, 169 %, 164 %, and 159 % for deflection angles of 0, 30, 60, and 90, respectively. Because the increase in porosity from 0.93 to 0.98 has led to a 16 % increase in permeability. Also, increasing the porosity according to the momentum equation has reduced the effects of advective and viscous terms. In addition, this increment of porosity enhances the maximum temperature by $33.5, 33.2, 29.9 and 29.5K$ for the deflection angles of 0, 30, 60 and 90, respectively. Although, the increase in porosity has led to an increase in convective heat transfer (due to the increase in flow velocity), but the effects of the decrease in effective thermal conductivity due to the increase in porosity have been predominant. According to the second column of Fig. 4, enhancing the deflection angle causes the isotherms to tilt slightly in the opposite direction of the gravitational acceleration as opposed to the 0.93 porosity. Because in this porosity (0.98), the effects of convective heat transfer have been slightly increased compared to the 0.93 porosity. Also, although the velocity and temperature counters in Fig. 4 are generally similar to Fig. 3, the maximum values of flow velocity and temperature inside the chamber are different from each other, which can be examined as following. Increasing the deflection angle from 0 to 30, 60 and 90 increased the maximum flow velocity by 57.7, 87.7 and 88.1 %, respectively. In addition, escalating the deflection angle from 0 to 30, 60 and 90 reduced the maximum temperature by $0.3, 0.6 and 1K$, respectively. To complete the explanation, it can be stated that enhancing the porosity from 0.93 to 0.98 has enhanced the convective heat transfer, but still, the effects of the conductive heat transfer due to the high thermal conductivity of the nickel porous medium are predominant.

Fig. 5 demonstrates the melting fraction contours of the molten NEPCM inside the chamber for a volume fraction of 6 %. As mentioned, the fusion temperature of NEPCM's core is $316.7K$. At 0.93 porosity, very small volumes of NEPCM particles are melted near the hot plate. But, the volume of melted NEPCM particles is greater at 0.98 porosity. Because 0.93 porosity keeps the chamber temperature significantly lower than that of 0.98 porosity due to having high effective thermal conductivity, hence, NEPCM particles are not exposed to or above the melting point. Also, increasing the deflection angle has no effect on the appearance of the melting fraction in a 0.93 porosity, but the melting fraction in a 0.98 porosity tends to move in the opposite direction of gravity acceleration. Because to be melted NEPCM is a function of temperature, the melting fraction behavior follows the temperature counters.

Finally, we can talk about the important parameter of average Nusselt number, which is ratio of convective to conductive heat transfer. Therefore, Fig. 6 is presented to study the effects of porosity number, deflection angle, and volume fraction of NEPCM on the average Nusselt number. According to Fig. 6a, the increase in volume fraction led to an enhance in convective heat transfer due to an increase in the specific heat capacity of the mixture, resulting in an increase in the average Nusselt number. But, the deflection angle does not affect the average Nusselt number. Because, as argued for the 0.93 porosity, the thermal conductivity effects of the nickel porous medium prevail over the effects of the flow pattern change. Also, according to porosity 0.98 (Fig. 6b), adding NEPCM increases the average Nusselt number - as described above. In addition, enhancing the deflection angle from 0 to 90 has

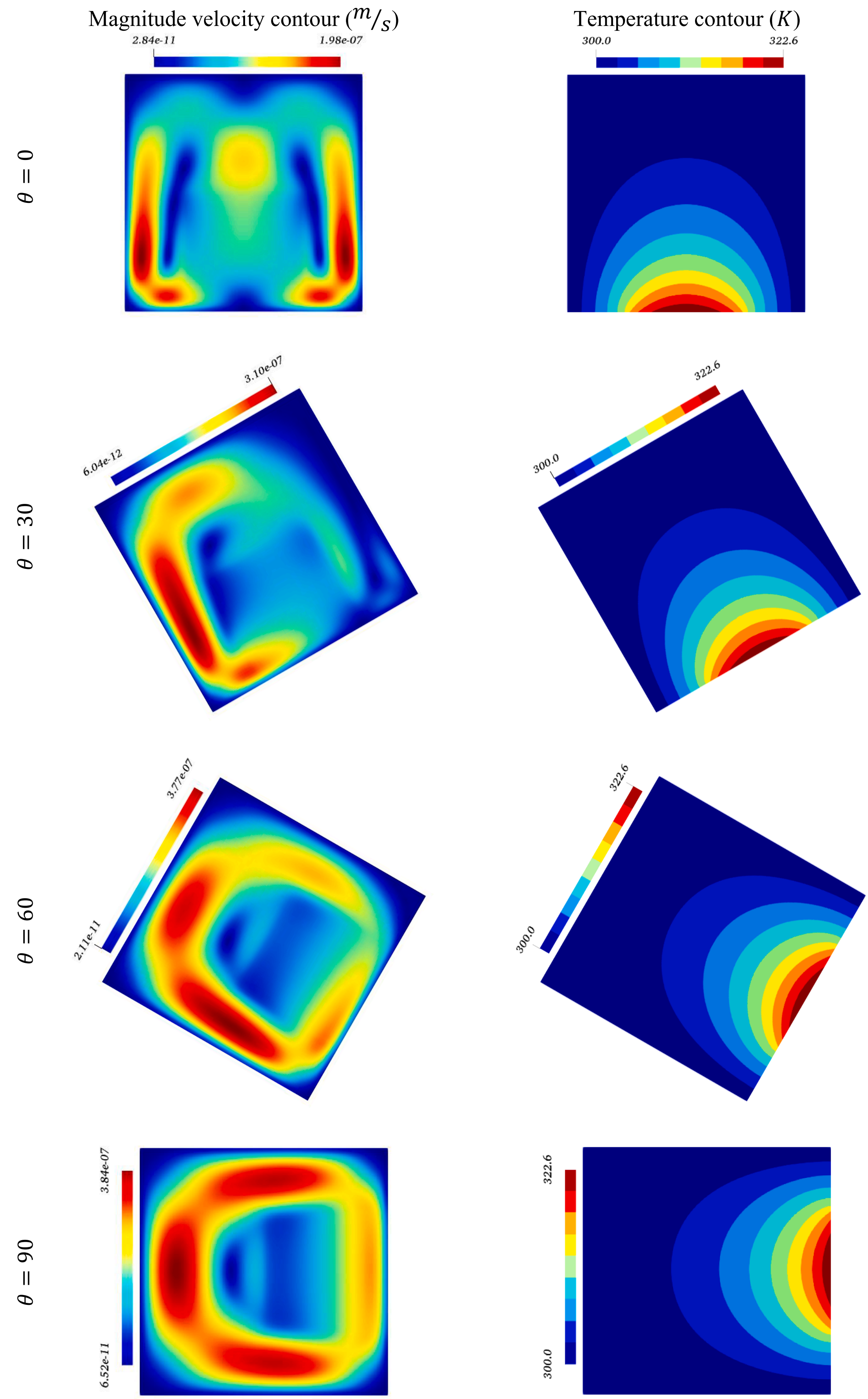

Fig. 3. The magnetic velocity and temperature contours at conditions of $\varepsilon = 0.93 and \varphi = 6\%$.

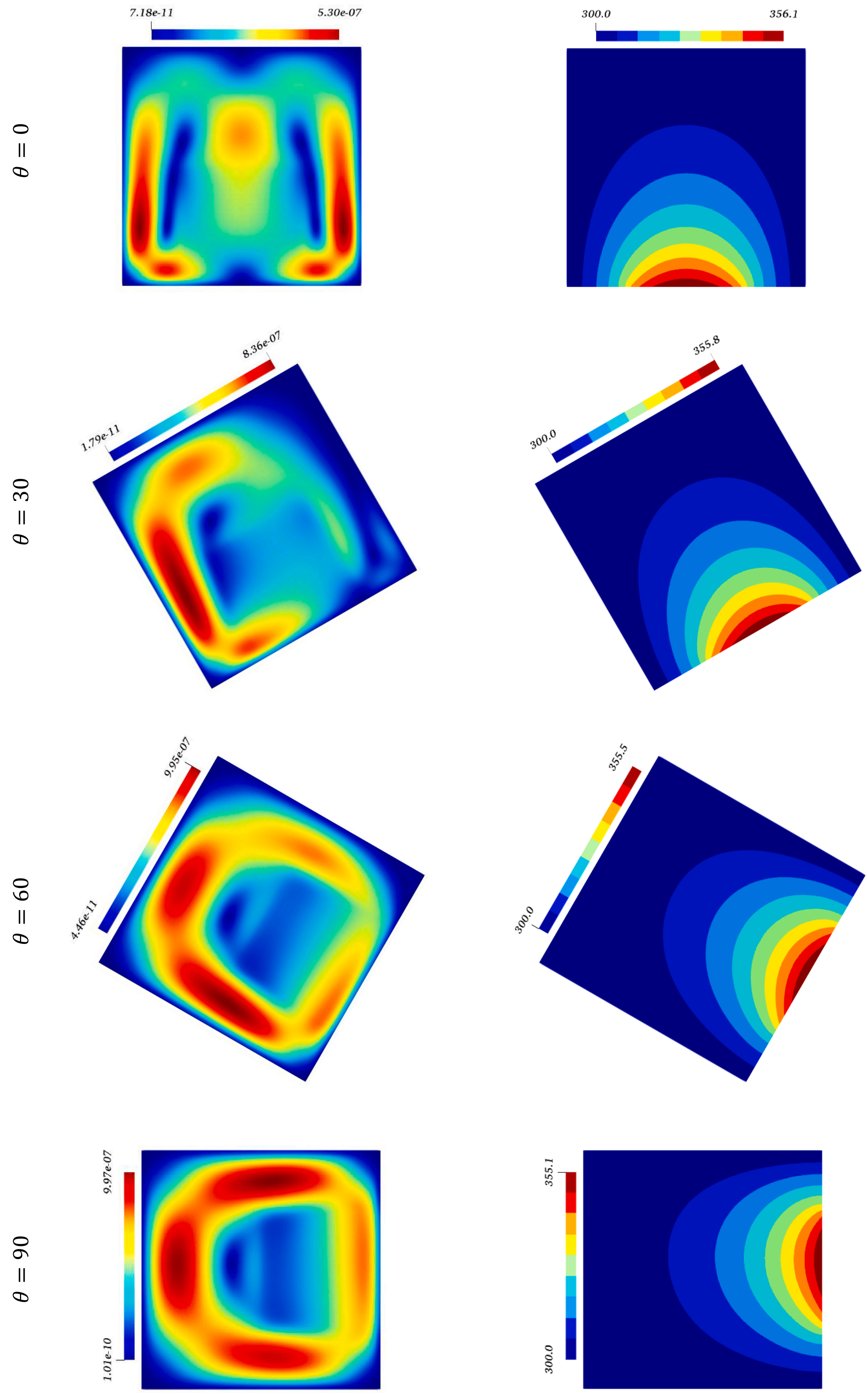

Fig. 4. The magnetic velocity and temperature contours at conditions of $\varepsilon = 0.98 and \varphi = 6\%$.

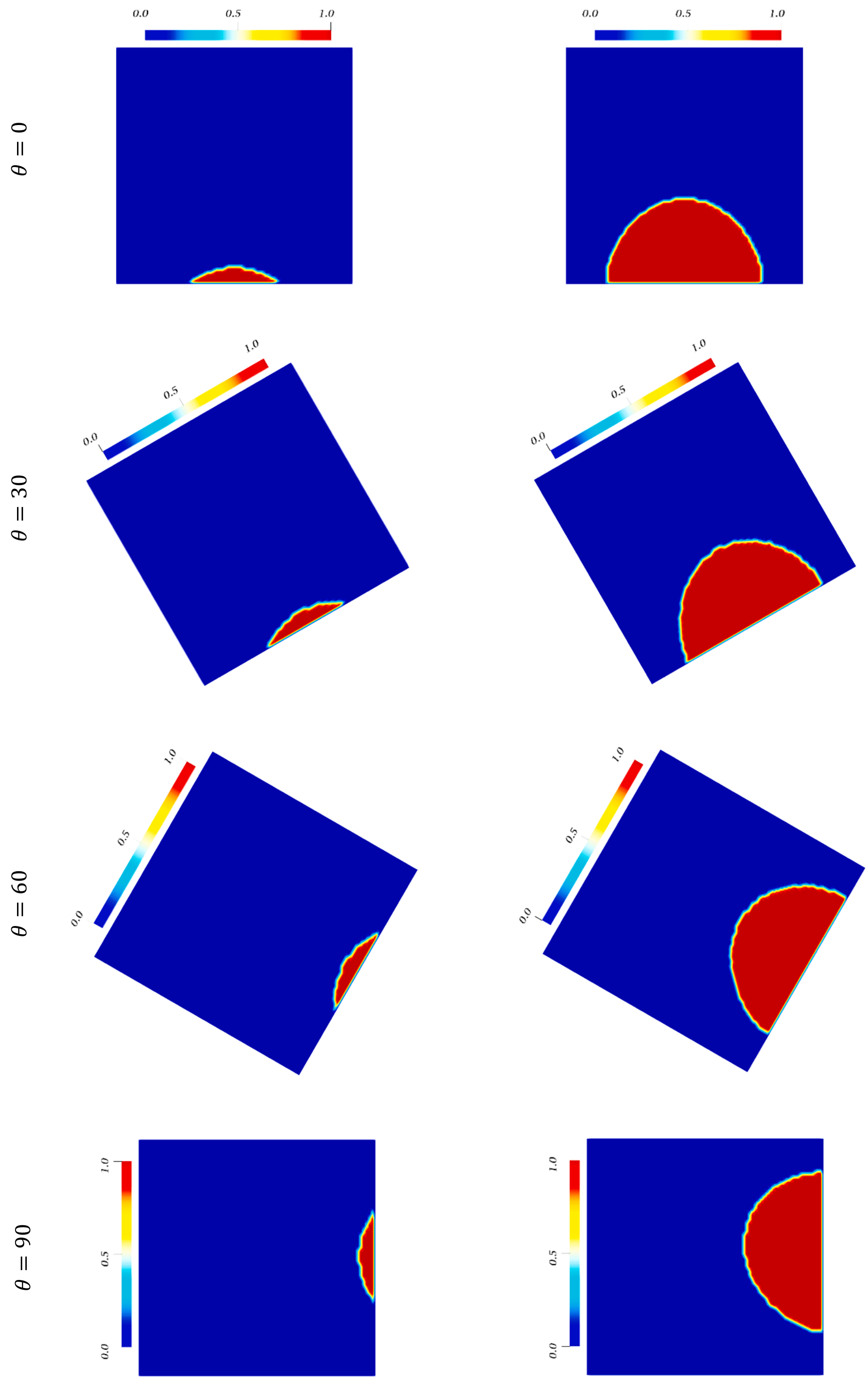

Fig. 5. The molten NEPCM contour at condition of $\varphi = 6\%$.

increased the average Nusselt number because, as previously argued (Fig. 4), increasing the deflection angle increased the flow velocity near the hot plate - it is noteworthy that in the convective heat transfer of 0.98 porosity is higher than 0.93 porosity. Also, by comparing the two porosity, it can be seen that the reduction of the porosity from 0.98 to 0.93 had a significant effect on the average Nusselt number because the effective thermal conductivity has been enhanced by 144 %.

Conclusion

This study simulated free convection within a cavity that can deviate counterclockwise. A hot plate with uniform heat flux at its bottom was cooled by the constant temperature walls. A nickel foam was used to strengthen heat transfer and placed on the hot plate. NEPCM particles with n-Docosane core were added to pure water to improve

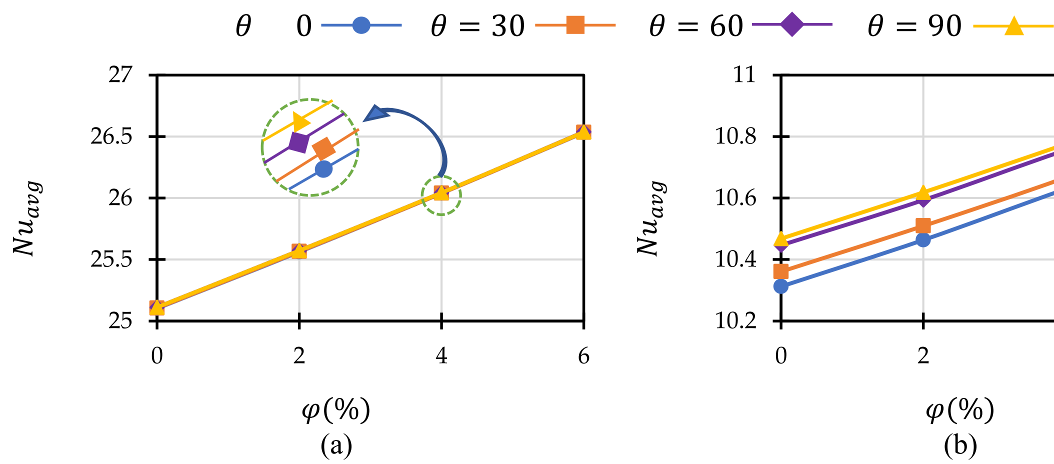

Fig. 6. The average Nusselt number for a) $\varepsilon = 0.93$ and b) $\varepsilon = 0.98$ at 10^5 Rayleigh number.

thermophysical properties of the cooling fluid. The study investigated the effects of porosity, deflection angle, and volume fraction of NEPCM in detail. Finally, to conclude this study, it can be said that, an increase in the volume fraction from 0 to 6 % led to an increase of 5.6 % in the average Nusselt number in a 0.93 porosity. Moreover, the addition of a 6 % volume fraction of NEPCM changed the averaged Nusselt number for the deflection angles of 0, 30, 60, and 90 by 4.55, 4.63, 4.58, and 4.56 % in the 0.98 porosity, respectively. eventually, the reduction of the porosity from 0.98 to 0.93 has strengthened the average Nusselt number by more than 142 %.

CRediT authorship contribution statement

Kamel Guedri: Writing – review & editing. **Fahid Riaz:** Investigation, Writing – review & editing. **Bandar M. Fadhl:** Investigation, Writing – review & editing. **Manoj Kumar Agrawal:** Investigation, Writing – review & editing. **Nehad Ali Shah:** Investigation. **Basim M. Makhdoum:** Investigation, Writing – review & editing. **Hossein Mehdizadeh Youshanlouei:** Conceptualization, Data curation, Software.

Declaration of Competing Interest

The authors declare that they have no known competing financial interests or personal relationships that could have appeared to influence the work reported in this paper.

Data availability

The authors do not have permission to share data.

Acknowledgments

- Authors acknowledge financial support from Abu Dhabi University's Office of Research and Sponsored Programs.
- The authors would like to thank the Deanship of Scientific Research at Umm Al-Qura University for supporting this work by Grant Code: (23UQU4331317DSR001).

References

[1] M. Stadler, W. Krause, M. Sonnenschein, U. Vogel, Modelling and evaluation of control schemes for enhancing load shift of electricity demand for cooling devices, Environ. Model. Softw. 24 (2) (2009) 285–295.

[2] N. Shirani, D. Toghraie, S. Rostami, Comparative study of mixed convection heat transfer of water–Cu nanofluid in an enclosure having multiple rotating circular cylinders with different configurations and considering harmonic cylinders rotation, J. Therm. Anal. Calorim. 144 (4) (2021) 1557–1570.

[3] K.A.M. Alharbi, M.N. Alshahrani, N. Ullah, N.M. Khan, K. Marek, A.A.A. Mousa, S. Ali, Cattaneo-Christov heat flow model for copper–water nanofluid heat transfer under Marangoni convection and slip conditions, Sci. Rep. 12 (1) (2022) 5360.

[4] B. Yang, P. Wang, A. Bar-Cohen, Mini-contact enhanced thermoelectric cooling of hot spots in high power devices, IEEE Trans. Compon. Packag. Technol. 30 (3) (2007) 432–438.

[5] N. Shirani, D. Toghraie, Numerical investigation of transient mixed convection of nanofluid in a cavity with non-Darcy porous inner block and rotating cylinders with harmonic motion, Sci. Rep. 11 (1) (2021) 17281.

[6] A. Shahsavar Goldanlou, M. Zarringhalam, N. Shirani, A. Alizadeh, D. Toghraie, S. Rostami, Investigation the effects of an external driving force and cone shape of roughness on the phase change behavior of Argon fluid within a microchannel by molecular dynamic simulation, J. Mol. Liq. 313 (2020), 113503.

[7] T. Yuge, Experiments on heat transfer from spheres including combined natural and forced convection, J. Heat Transf. (US) 82 (3) (1960) 214–220.

[8] S.M. Saleh Mousavi-Bafrouyi, R. Eslami-Farsani, A. Geranmayeh, The temperature effects on the mechanical properties of pseudo-ductile thin-ply unidirectional carbon-basalt fibers/epoxy hybrid composites with different stacking sequences, Fibers Polym. 22 (11) (2021) 3162–3171.

[9] G. Yan, A. Shawabkeh, R. Chaturvedi, R. Nur-Firyal, M. Mehdizadeh Youshanlouei, Using MHD free convection to receive the generated heat by an elliptical porous media, Case Stud. Therm. Eng. 36 (2022), 102153.

[10] J.L. Liu, X.Q. Feng, G.F. Wang, Buoyant force and sinking conditions of a hydrophobic thin rod floating on water, Phys. Rev. E 76 (6) (2007), 066103.

[11] A.R. Abdulmunem, P.M. Samin, H.A. Rahman, H.A. Hussien, H. Ghazali, A novel thermal regulation method for photovoltaic panels using porous metals filled with phase change material and nanoparticle additives, J. Storage Mater. 39 (2021), 102621.

[12] S. Dong, K. S Al-Zahrani, S. A Reda, K. Sharma, M. Talal Amin, E. Tag-Eldin, M. Mehdizadeh Youshanlouei, Investigation of thermal performance of a shell and tube latent heat thermal energy storage tank in the presence of different nano-enhanced PCMs, Case Stud. Therm. Eng. 37 (2022), 102280.

[13] J.R. Bodoia, J.F. Osterle. 1962. The development of free convection between heated vertical plates.

[14] H. Wu, X. Wu, L. Feng, M. Mehdizadeh Youshanlouei, Cooling a central processing unit by installing a mini channel and flowing nanofluid, and investigating economic efficiency, Case Stud. Therm. Eng. 30 (2022), 101719.

[15] S. Mirshahi, O. Rajabi, A mathematical model based on an adaptive neuro-fuzzy inference system for matrixes including indomethacin, J. Appl. Pharm. 9 (58) (2018) 1–6.

[16] S.Y. Motlagh, E. Golab, A.N. Sadr, Two-phase modeling of the free convection of nanofluid inside the inclined porous semi-annulus enclosure, Int. J. Mech. Sci. 164 (2019), 105183.

[17] F. Faily, H. Shafeie, O. Abouali, 2011, January. Comparison of the effect of embedded grooves on the heat removal and pressure drop in microchannel heat sinks. In International Conference on Nanochannels, Microchannels, and Minichannels (Vol. 44632, pp. 679-684).

[18] A.S. Tajani, A. Haghighizadeh, V. Soheili, S. Mirshahi, O. Rajabi, In vitro bioequivalence study of 8 generic and 3 brands of sertraline-HCl tablets in Iran market, Biomed. Pharmacol. J. 10 (3) (2017) 1109–1116.

[19] B. Vahedi, E. Golab, A. Nasiri Sadr, K. Vafai, Thermal, thermodynamic and exergoeconomic investigation of a parabolic trough collector utilizing nanofluids, Appl. Therm. Eng. 206 (2022), 118117.

[20] M. Mesgarpour, A. Heydari, S. Wongwises, M.R. Gharib, Numerical optimization of a new concept in porous medium considering thermal radiation: Photovoltaic panel cooling application, Sol. Energy 216 (2021) 452–467.

[21] J. Duan, A novel heat sink for cooling concentrator photovoltaic system using PCM-porous system, Appl. Therm. Eng. 186 (2021), 116522.

[22] T. Brahim, A. Jemni, CFD analysis of hotspots copper metal foam flat heat pipe for electronic cooling applications, Int. J. Therm. Sci. 159 (2021), 106583.

[23] Y. Mona, T.A. Do, S. Pothaya, S. Wongnor, The effect of porous media on a solar thermoelectric energy harvesting system, Energy Rep. 7 (2021) 493–498.

[24] A. Aydın, T. Engin, H. Yasar, A. Yeter, A.H. Perut, Computational fluid dynamics analysis of a vehicle radiator using porous media approach, Heat Transfer Eng. 42 (11) (2021) 904–916.

[25] A.R. Abdulmunem, P.M. Samin, H.A. Rahman, H.A. Hussien, I.I. Mazali, Enhancing PV Cell's electrical efficiency using phase change material with copper foam matrix and multi-walled carbon nanotubes as passive cooling method, Renew. Energy 160 (2020) 663–675.

[26] A.R. Abdulmunem, P.M. Samin, H.A. Rahman, H.A. Hussien, I.I. Mazali, H. Ghazali, Numerical and experimental analysis of the tilt angle's effects on the characteristics of the melting process of PCM-based as PV cell's backside heat sink, Renew. Energy 173 (2021) 520–530.

[27] A.R. Abdulmunem, P.M. Samin, H.A. Rahman, H.A. Hussien, I.I. Mazali, H. Ghazali, Experimental and numerical investigations on the effects of different tilt angles on the phase change material melting process in a rectangular container, J. Storage Mater. 32 (2020), 101914.

[28] E. Golab, B. Vahedi, A. Jain, R.A. Taylor, K. Vafai, Laminar forced convection in a tube with a nano-encapsulated phase change materials: minimizing exergy losses and maximizing the heat transfer rate, J. Storage Mater. 65 (2023), 107233.

[29] W.Q. Li, S.J. Guo, L. Tan, L.L. Liu, W. Ao, Heat transfer enhancement of nano-encapsulated phase change material (NEPCM) using metal foam for thermal energy storage, Int. J. Heat Mass Transf. 166 (2021), 120737.

[30] M.S. Ghoghaei, A. Mahmoudian, O. Mohammadi, M.B. Shafii, H. Jafari Mosleh, M. Zandieh, M.H. Ahmadi, A review on the applications of micro-/nano-encapsulated phase change material slurry in heat transfer and thermal storage systems, J. Therm. Anal. Calorim. 145 (2) (2021) 245–268.

[31] H. Saleh, Z. Siri, M. Ghalambaz, Natural convection from a bottom heated of an asymmetrical U-shaped enclosure with nano-encapsulated phase change material, J. Storage Mater. 38 (2021) 102538.

[32] Z. Raizah, A.M. Aly, Double-diffusive convection of a rotating circular cylinder in a porous cavity suspended by nano-encapsulated phase change materials, Case Stud. Therm. Eng. 24 (2021), 100864.

[33] W. Lan, B. Shang, R. Wu, X. Yu, R. Hu, X. Luo, Thermally-enhanced nanoencapsulated phase change materials for latent functionally thermal fluid, Int. J. Therm. Sci. 159 (2021), 106619.

[34] A.J. Torregrosa, A. Broatch, P. Olmeda, A. Dreif, Assessment of the improvement of internal combustion engines cooling system using nanofluids and nanoencapsulated phase change materials, Int. J. Engine Res. 22 (6) (2021) 1939–1957.

[35] M.R. Faraz, H. Ahmadi, G. Liaghat, S. Vahid, O. Razmkhah, A. Tarafdar, Energy absorption assessment of bio-mimicked hybrid Al/PP sandwich tube: experimental and Numerical Investigation, Thin-Walled Struct. 181 (2022), 110116.

[36] R. Syah, A. Davarpanah, M. Elveny, D. Ramdan, Natural convection of water and nano-emulsion phase change material inside a square enclosure to cool the electronic components, Int. J. Energy Res. 46 (3) (2022) 2403–2417.

[37] E. Golab, S. Goudarzi, H. Kazemi-Varnamkhasti, H. Amigh, F. Ghaemi, D. Baleanu, A. Karimipour, Investigation of the effect of adding nano-encapsulated phase change material to water in natural convection inside a rectangular cavity, J. Storage Mater. 40 (2021), 102699.

[38] H. Hamzah, A. Albojamal, B. Sahin, K. Vafai, Thermal management of transverse magnetic source effects on nanofluid natural convection in a wavy porous enclosure, J. Therm. Anal. Calorim. 143 (3) (2021) 2851–2865.

[39] K. Abdulkhaliq M Alharbi, O. Aldosari, N. Sina, H.Ş. Aybar, S. Fuxi, S.E. Alkhatib, A. Allah A Mousa, Installation of rectangular enclosures filled with phase change nanomaterials on the thrombus walls of a residential building to manage solar radiation in different seasons of the year, J. Build. Eng. 57 (2022), 104732.

[40] I. Chabani, F. Mebarek-Oudina, H. Vaidya, A.I. Ismail, Numerical analysis of magnetic hybrid Nano-fluid natural convective flow in an adjusted porous trapezoidal enclosure, J. Magn. Magn. Mater. 564 (2022), 170142.

[41] Y.D. Reddy, F. Mebarek-Oudina, B.S. Goud, A.I. Ismail, Radiation, velocity and thermal slips effect toward MHD boundary layer flow through heat and mass transport of Williamson nanofluid with porous medium, Arab. J. Sci. Eng. 47 (12) (2022) 16355–16369.

[42] M. Hassan, F. Mebarek-Oudina, A. Faisal, A. Ghafar, A.I. Ismail, Thermal energy and mass transport of shear thinning fluid under effects of low to high shear rate viscosity, Int. J. Thermofluids 15 (2022), 100176.

[43] Q. Lou, B. Ali, S.U. Rehman, D. Habib, S. Abdal, N.A. Shah, J.D. Chung, Micropolar dusty fluid: coriolis force effects on dynamics of MHD rotating fluid when Lorentz force is significant, Mathematics 10 (15) (2022) 2630.

[44] S. Kavya, V. Nagendramma, N.A. Ahammad, S. Ahmad, C.S.K. Raju, N.A. Shah, Magnetic-hybrid nanoparticles with stretching/shrinking cylinder in a suspension of MoS_4 and copper nanoparticles, Int. Commun. Heat Mass Transf. 136 (2022), 106150.

[45] N.A. Shah, A. Wakif, R. Shah, S.-J. Yook, B. Salah, Y. Mahsud, K. Hussain, Effects of fractional derivative and heat source/sink on MHD free convection flow of nanofluids in a vertical cylinder: a generalized Fourier's law model, Case Stud. Therm. Eng. 28 (2021), 101518.

[46] J. Luo, I.B. Mansir, K. Sharma, I. Mahariq, F. Jarad, M.M. Youshanlouei, H. Moria, F. Aldawi, S.A. Reda, Profit and efficiency enhancement of a cylindrical solar collector by structural modification of helical tube, Case Stud. Therm. Eng. 34 (2022), 101982.